Large Eddy Simulation Study of H2/CH4 Flame Structure at MILD Condition

Y. Afarin*, S. Tabejamaat* and A. Mardani[*]
Yashar-afarin@aut.ac.ir

*Department *of* Aerospace Engineering, Amirkabir University *of* Technology, Tehran, Iran

Abstract
This paper demonstrates the large eddy simulation (LES) of a H2/CH4 jet in a hot and diluted co-flow stream which emulated the MILD combustion regime. The turbulence-combustion interaction is modeled using the CPaSR model while the reduced chemical mechanism of DRM-22 represents the chemical reactions. Structure of MILD combustion regime for two co-flow oxygen concentration of 3 and 9% (by mass) are investigated. The reaction zone structure is shown by the temperature distribution and distribution of OH, CH_2O and HCO mass fraction. Results show that the measurements are predicted with an acceptable accuracy. Moreover, the extinction and re-ignition phenomena that take place under this combustion regime is captured by the current numerical method. The later phenomena occur in a larger zone by decreasing the O_2 concentration as well as the reaction zone expands.

Introduction
Rapid industrial development during recent decades in addition to problems related to global warming and reduction in fossil energy resources criticized the current situation. In this circumstances utilizing new technology seems to be critically necessary in order to decrease pollutions and increase the combustion efficiency. MILD (Moderate or Intense Low-oxygen Dilution) combustion [1] is a promising candidate for replacing the old combustion technology due to its specific characteristics consist of increasing thermal efficiency and decreasing the pollution emission. This technology has been successfully applied in several industries [2] but doing more studies are necessary to investigate its combustion characteristics [1,3].
To emulate MILD combustion regime, Dally et al. [3] designed and used a burner in which a jet of fuel (CH_4 / H_2) is injected in hot coflow oxidant stream. In their research influence of different O_2 mass fraction coflow on flame structure at different location from the nozzle were studied. Their experimental results were used by some other researchers as a reference to assess their numerical results. Among them, Christo et al. [4] compared various turbulence chemistry interaction models and also qualified the k-ε model in MILD combustion. They also reported that, MILD combustion modeling is beyond the capability of single conserved scalar-based models. Frassoldati et al. [5] studied different modeling approaches on flame structure prediction in MILD combustion by using FLUENT. According to their result the accuracy of the numerical solution, especially for the turbulent intensity, is sensitive to the boundary conditions. Mardani et al. [6] clarify the importance of differential diffusion method on flame structure under MILD combustion conditions. They showed that the molecular transportation has a strong effect on flame structure. LES modeling of MILD combustion regime was performed by Ihme et al. [7] where they used a presumed probability density

function to model the turbulent chemistry interaction on unresolved scales. They discussed the importance of variations in scalar inflow conditions on turbulent combustion under MILD combustion regime. They found that LES modeling has the capability to be used in this regime but boundary conditions could have a significant effect on the final results.
Kobayashi et al. [8] experimentally investigate the flame structure under high temperature air combustion. They found that flow turbulence have a profound effect in decreasing NOx emission. Also, according to their result the turbulence is the main factor of OH suppressions and local flame extinctions. In this regard, Medwell et al. [9] investigated the effect of fuel Reynolds number on MILD flame structure. According to their results, increasing the Reynolds number intensifies the convolution and weakening the OH distribution. Obviously from the above researches, turbulence has the important effect on local flame suppression.
In the MILD combustion regime, the mean flow velocity is high to provide a combustible mixture with low oxygen level and which also prevents the hot spots in combustion chamber. It is necessary to have both extinction and re-ignition, especially near the nozzle exit zone, in order to have the MILD combustion condition. Such local extinction and re-ignition are investigated experimentally by Kobayashi et al. [8]. Numerical investigations of the MILD combustion by Christo et al. [4] and Mardani et al. [6] are indicated that although the effect of turbulence on controlling the flame is important, the influence of finite rate chemistry never can be negligible in MILD regime. Based on the above mentioned researches, turbulence chemistry interaction has a profound effect on the numerical results at MILD combustion.
Many investigations have been performed to study turbulent chemistry modeling at MILD combustion. Among them, the Eddy Dissipation Concept [10], EDC, model has the possibility to couple CFD simulation and detailed kinetic more simply than other models. Therefore there was a great interest to use this model specially when the computational cost is high. Christo et al. [4], Mardani et al. [6] and Frassoldati et al. [5] used EDC and reported the reasonably accurate results compared with experimental measurements. In all of these researches $k-\epsilon$ model were used as the turbulence model.
In the current research, flame structure under MILD combustion regime is investigated. For the first time, combination of large eddy simulation to model turbulence quantity and a modified version of EDC referenced by Chalmers Partially Stirred Reactor Model (CPaSR), Chomiak and Karlsson [11], is considered to calculate the turbulence-chemistry interactions. This study focuses on experimental measurements of Dally et al. [3]. The purpose of this study is discussing about local flame extinction under MILD combustion regime.

Numerical Method and Governing Equations

In this paper, compressible Navier-Stokes equations (NSE) is used to describe the flow. In Large Eddy Simulation, filtering the dependent variables divide them into GS and SGS components in a way that $V=\tilde{V}+V^{"}$, where $\tilde{V}$ is resolved part. In this study, box filter $\bar{\Delta}=(\Delta_x\Delta_y\Delta_z)^{1/3}$ is used to filter variables, where Δ_i refers to grid size in i direction. According to Favre approach a filtering operation is weighted by the density according to following the equation:

$$\tilde{f}=\rho\bar{f}/\bar{\rho} \qquad (1)$$

By filtering the variables in compressible NSE and using the Smagoronisky model [12], the instantaneous balance filtered equations leads to the following equations. These equations formally are similar to Reynolds averaged balance equations [13]:

$$\frac{\partial \bar{\rho}}{\partial t} + \frac{\partial}{\partial x_i}(\bar{\rho}\widetilde{u_\iota}) = 0 \quad (2)$$

$$\frac{\partial \bar{\rho}\widetilde{Y_k}}{\partial t} + \frac{\partial}{\partial x_i}\left(\bar{\rho}\widetilde{u_\iota}\widetilde{Y_k}\right) = \frac{\partial}{\partial x_i}\left((\mu + \frac{\mu_{SGS}}{Sc_t})\frac{\partial \widetilde{Y_k}}{\partial x_i}\right) + \overline{\dot{\omega}_k} \quad k = 1, \dots, N \quad (3)$$

$$\frac{\partial \bar{\rho}\widetilde{u_\iota}}{\partial t} + \frac{\partial}{\partial x_i}\left(\bar{\rho}\widetilde{u_\iota}\widetilde{u_j}\right) + \frac{\partial \bar{p}}{\partial x_i} = \frac{\partial}{\partial x_i}\left(\overline{\tau_{\iota j}} + \mu_{SGS}\left(\frac{\partial \widetilde{u_\iota}}{\partial x_j} + \frac{\partial \widetilde{u_\iota}}{\partial x_i}\right) + \frac{\delta_{ij}}{3}T_{kk}\right) \quad (4)$$

$$\frac{\partial \bar{\rho}\tilde{h}}{\partial t} + \frac{\partial}{\partial x_i}\left(\bar{\rho}\widetilde{u_\iota}\tilde{h}\right) = \frac{\overline{Dp}}{Dt} + \frac{\partial}{\partial x_i}\left((\frac{\mu}{Pr} + \frac{\mu_{SGS}}{Pr_t})\frac{\partial \tilde{h}}{\partial x_i}\right) \quad (5)$$

where u is the velocity vector, p is the pressure, ρ is the flow density, h is the enthalpy and Y_i is the mass fraction of ith species. The isotropic contribution, T_{kk}, in equation (which is twice the subgrid scale turbulent kinetic energy) is unknown and usually absorbed into the filtered pressure [13]. In the above equations Sc_t and Pr_t are considered as unity. All terms in above equations are closed except the species transport's (Eq. 3) source term. The μ_{SGS} is the sub-grid scale viscosity which is computed according to the below mentioned equation:

$$\mu_{SGS} = \bar{\rho}C_k\sqrt{k}\Delta \quad (6)$$

where C_k is set to 0.02 in this study. The term ε_{SGS} is defined as:

$$\varepsilon_{SGS} = \frac{C_e k\sqrt{k}}{\Delta} \quad (7)$$

where C_e is constant and set to 1.048.

In the present study, the OpenFOAM (Open Field Operation and Manipulation) CFD toolbox is used to solve transport equations. OpenFOAM is a package of free and open source object oriented C++ codes, Weller et.al [14]. The PISO (Pressure Implicit with Splitting of Operators) method [15] is used to solve NSE in an unsteady configuration. Its preference is due to two factors. This method needs no under-relaxation and the momentum corrector step is recalled more than one time. Briefly this solver is based on unsteady PISO with two pressure correctors and two momentum correctors with time step $10^{-6}s$ and convergence criteria for residuals 10^{-11}. For more information about how OpenFOAM uses this procedure, one may refer to Ref. [16]. The implicit first order bounded Euler scheme is used to discrete the unsteady term. The convection and diffusion terms are discretized using the Normalized Variable Diagram (NVD) Scheme and the second order central difference schemes, respectively. Mass flux calculation is done by Linear (second order central difference) interpolation.

In the present study, modified version of the *reactingFoam* (change from RANS to LES) that is one of the reacting flow solvers of OpenFOAM is used. This solver uses the CPaSR as a turbulent chemistry interaction model. Indeed, the basic difference between EDC and CPaSR is in computing approach of the chemical timescale. In CPaSR model, the flame thickness is assumed to be much thinner than usual computational cell, therefore cell space should be split into two parts; reacting part and non-reacting part. The theory postulate that in reacting part, like a perfectly stirred reactor, all species are perfectly stirred and react during reaction time. After reactions takes place, the species (burned and unburned) are assumed to

be mixed due to turbulence during mixing time, τ_{mix}, and then final concentration is composed of burned and unburned species. The important information lies in defining mixing time, τ_{mix}, chemical time scale, τ_c, and description of each computational cell division process. The chemical time scale,τ_c, is determined by solving the reaction system's fully coupled ODEs, and finding the characteristic time for that system. The turbulence mixing time is related to effective viscosity, mean density, and sub-grid scale turbulent dissipation according to the below equation:

$$\tau_{mix} = C_{mix}\sqrt{\frac{(\mu + \mu_{SGS})}{\bar{\rho}\varepsilon_{SGS}}} \quad (8)$$

where $C_{mix} = 1$. In all above expressions k is SGS kinetic energy.

Rate of reaction for specie i can be scaled by reactive volume fraction κ, as:

$$\frac{\partial C^i}{\partial t} = \frac{C_1^i - C_o^i}{\tau} = \kappa\, RR_i(C_1^i) \quad (9)$$

where τ is the residence time (numerical time step), C_0^i is defined as initial concentration of species i in a control volume, C_1^i is final concentration of species i in a control volume, and κ (kappa) which takes a value between 0 to 1 is defined as:

$$\kappa = \frac{\tau_c + \tau}{\tau_c + \tau_{mix} + \tau} \quad (10)$$

One of the most important parameter in current study that can be used to clarify the turbulent and chemistry interaction is κ. This factor changes the species transport equation as below:

$$\frac{\partial \rho Y_i}{\partial t} + \nabla(\rho Y_i U) - \nabla\left(\mu_{eff}\nabla(Y_i)\right) = S_i + \kappa RR_i(C_i) \quad (11)$$

Based on its definition, the value of this term is one, for a control volume without any reactions or where the chemical timescale is much larger than the mixing time scale, ($\tau_c \gg \tau_{mix}$). But in situations that the process of mixing and reaction have the same time scale orders, this term has the value lower than one. Thus briefly, by increasing the turbulence intensity and thereby decreasing the τ_{mix}in reaction zone, κ approaches to unity.

It should be noted that this model is different from the stochastic one which is based on a simplified joint composition probability density function transport equation and is known as PaSR model.

The 3D computational domain is constructed according to the experimental burner geometry of Dally et al. [3]. It is a H_2/CH_4 jet in Hot Co-flow (JHC) mounted in a wind tunnel with an air flows of 3.2 $^{m}/_{s}$ parallel to the burner axis. The JHC burner consists of a fuel and a hot coflow jet which are mounted in a wind tunnel with air flows (23% O_2+77% N_2 (mass basis)). Fig. 1 shows different sections of the Dally et.al [3] burner, schematically.

Inlet boundary conditions, for mean species mass fractions and mean velocity profiles, are set using the results of a separate modeling at upstream of burner exit plane. The mean inlet velocity of hot co-flow mixture and wind tunnel air are 3.2 m/s and the mean inlet velocity of

fuel jet is around 100 m/s. The inlet temperature of fuel mixture, hot co-flow mixture and air are 305, 1300 and 300 K, respectively. The inlet Reynolds number of fuel mixture on the basis of fuel mixture jet velocity and temperature is approximately equal to 10000. Mardani et al. [6], Christo et al. [4] and Frassoldati et al. [5] reported that the results are not sensible to turbulence intensity at the hot co-flow and wind tunnel, but the value of turbulent intensity of the fuel inlet has very significant effect on numerical results. Because the value of turbulent intensity of fuel inlet was not indicated by Dally et al. [3], different researchers used different values of fuel inlet turbulent intensity. For instance, although the experimentally measured turbulent kinetic energy is reported as 16 m^2/s^2 at the fuel inlet by Christo et al. [4], they preferred to use mean turbulent kinetic energy of 60 m^2/s^2 (7.5% turbulent intensity). Also, Mardani et al. [6] adjusted it to 7% in order to have a better agreement between the numerical and experimental results. In the present research, the turbulence intensity at the fuel inlet is set to 7%.

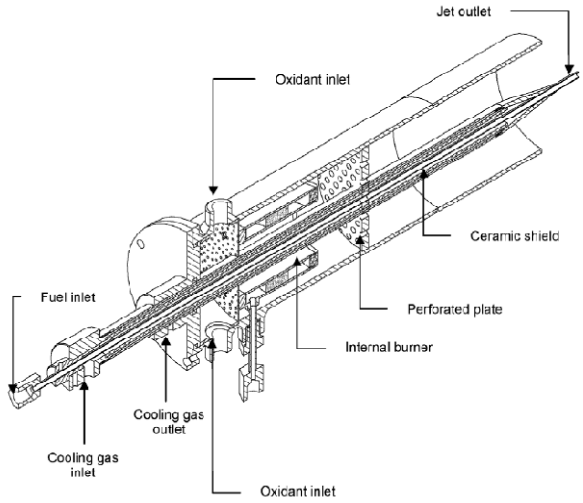

Figure 1. Schematic of Dally et al. [3] burner

A grid study with a number of control volumes approximately between 8×10^5 to 1.1×10^6 is performed and finally an unstructured grid with about 9×10^5 cells is selected. Detailed information about the cases are shown in Table 1. These cases are considered to study the effect of turbulence on flame structure on the MILD combustion characteristics of methane-hydrogen mixture at different co-flow oxygen content.

The DRM-22 chemical mechanism, [17], is considered for modeling of combustion reactions. It is a reduced mechanism of GRI 1.2 [18] with 22 species, including Ar and N2, for a total 104 reversible reactions. The results of Mardani et al.[6] show the good performance of the DRM-22 for computation chemical reactions under MILD combustion conditions.

Table 1. Specifications of numerical study

Case	Fuel Composition	Hot Oxidizer Composition	Chemical Mechanism
1	$20\%H_2+80\%CH_4$	$9\%O_2+6.5\%H_2O+5.5\%CO_2+79\%N_2$	DRM-22 [17]
2	$20\%H_2+80\%CH_4$	$3\%O_2+6.5\%H_2O+5.5\%CO_2+85\%N_2$	DRM-22 [17]

Numerical Results

Before any results discussion it is necessary to assess the quality of the LES method that is used in the present research. Klein [19] studied a method to evaluate large eddy simulation in the context of Implicit filtering. He declared that computing the numerical error in LES

method is more complicated in comparison with RANS. In LES method, the error is caused by two overlapping factors; subgrid parameterization and numerical contamination of the smaller retained structure [19]. Pope [20] demonstrated that a good LES should resolve at least 80% of the TKE. A new parameter was defined by [20] to present ratio of resolved to total kinetic energy:

$$resolved\ \ TKE\ ratio = \frac{k_{resolved}}{k_{resolved} + k_{SGS}} \qquad (12)$$

Fig. 2 illustrates *resolved TKE ratio* for flame with different percent of oxygen in different distances from the nozzle exit. As can be seen, in all cases, more than 94 % of total TKE was resolved directly and according to Ref. [20], results from the LES modeling with this characteristics could be reliable.

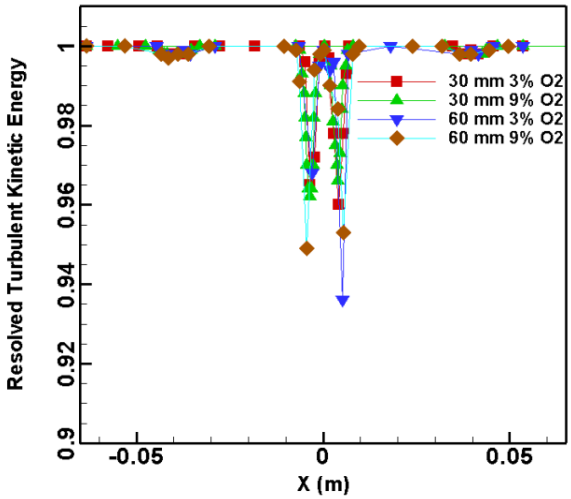

Figure 2. Resolved turbulent kinetic energy ration in case 1 and 2 in Table 1, on a line at 30 mm and 60 mm from the nozzle exit.

Dally's measurements [3], are used for validation of the results of the present study . Figs .3 and 4 shows distribution of CO, OH, CO_2 mass fraction and temperature versus mean mixture fraction at two distances, 30 mm and 60 mm, from the nozzle exit and for two 3% and 9%. percent of oxygen in co-flow. Mean mixture fraction (ξ), is calculated using the Bilger's [21] expression:

$$\xi = \left(\frac{2(\Gamma_C - \Gamma_{C,O})}{W_C} + \frac{(\Gamma_H - \Gamma_{H,O})}{2W_H} - \frac{(\Gamma_O - \Gamma_{O,O})}{W_O}\right) / \left(\frac{2(\Gamma_{C,F} - \Gamma_{C,O})}{W_C} + \frac{(\Gamma_{H,F} - \Gamma_{H,O})}{2W_H} - \frac{(\Gamma_{O,F} - \Gamma_{O,O})}{W_O}\right) \qquad (13)$$

In the above equation, Γ_i represent the value of conserved scalar that is given by mass fraction of element i and W_i is referred to the atomic mass of element i. Detailed information about computing Γ_i is resented at [21]. Also, according to Christo and Dally [4], the effect of thermal radiation on numerical results is considered negligible.

As can be seen from Figs. 3 and 4, the numerical and experimental results are in good agreement. Some differences in Figs. 3 and 4 could be referred to acceptable accuracy of chemical reaction calculations and flow dynamic modeling or may be experimental accuracy.

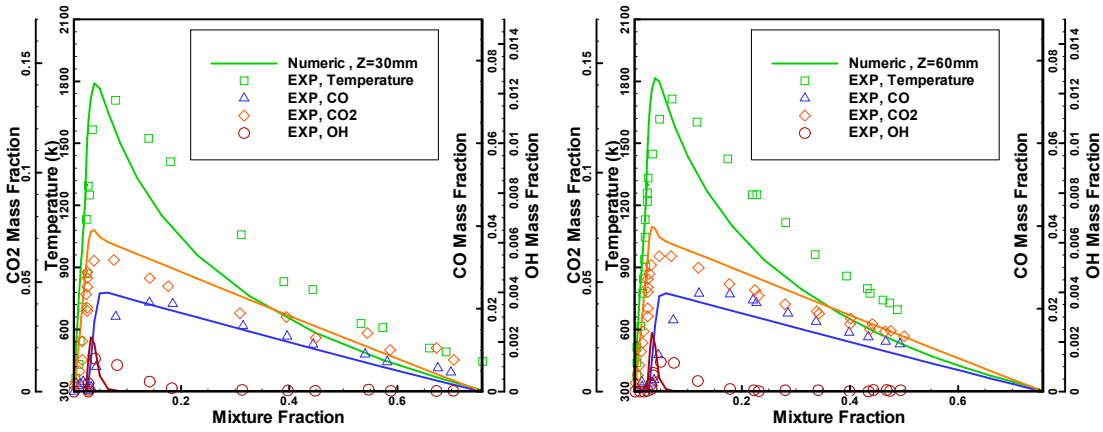

Figure 3. Distribution of CO, OH, CO_2 mass fraction and temperature versus mixture fraction (case 1 in Table 1) on a line at 30 mm (left) and 60 mm (right) from the nozzle exit.

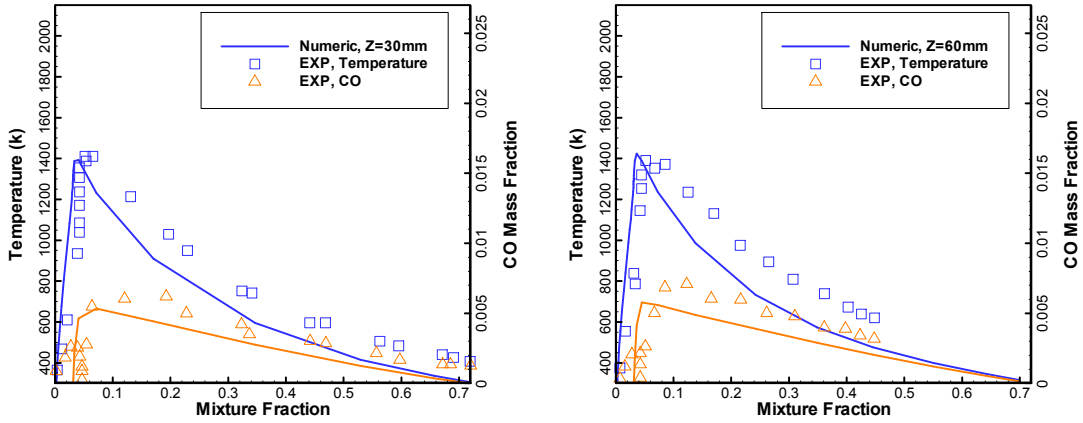

Figure 4. Distribution of CO, OH, CO_2 mass fraction and temperature versus mixture fraction (case 2 in Table 1) on a line at 30 mm (left) and 60 mm (right) from the nozzle exit..

Results for 9% O_2

In order to study the flame structure at MILD combustion, the contour of mean OH mass fraction and κ are presented in Figs. 5.a and 5.b respectively, for 9% of O_2 coflow. The location of two mixture fractions of 0.037 and 0.015 also are shown in this figure. The mixture fraction of 0.037 is stand for stoichiometric mixture. Apparently, there is a discrepancy between maximum value of OH mass fraction and the position where stoichiometric mixture fracture occurs. According to this figures, peak of OH mass fraction are in a zone where mixture fraction is less than stoichiometric value and is equal to 0.015.

The distribution of OH mass fraction shows that there is some local extinction in reaction zones especially near the fuel exit nozzle. This convolution and weakening in OH mass fraction were also reported by Medwell et al. [9] and Kobayashi et al. [8]. According to their

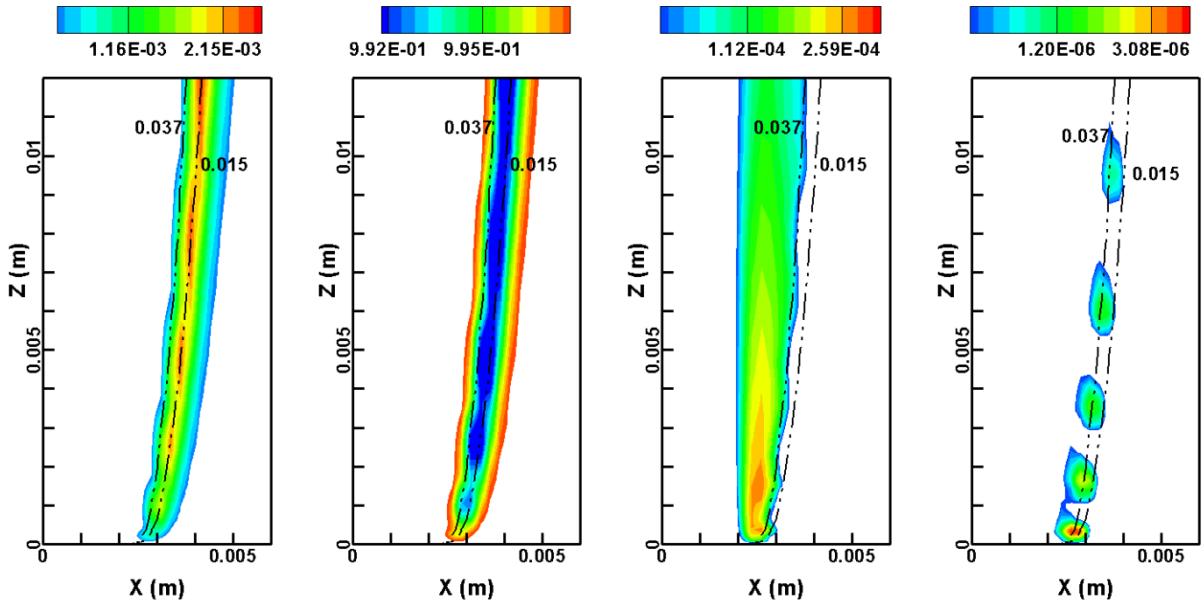

a. Contour of OH **b**. Contour of κ **c**. Contour of CH_2O **d**. Contour of HCO

Figure 5. Contour of κ and three other species mass fraction for 9% O_2 coflow

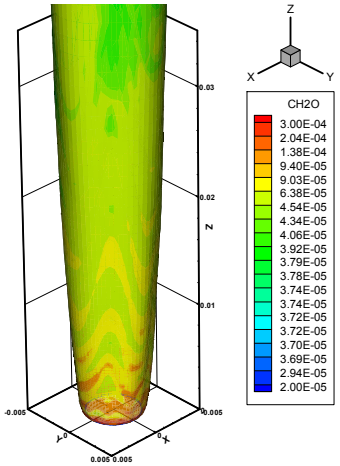

a. Contour of CH_2O, $\xi = 0.037$

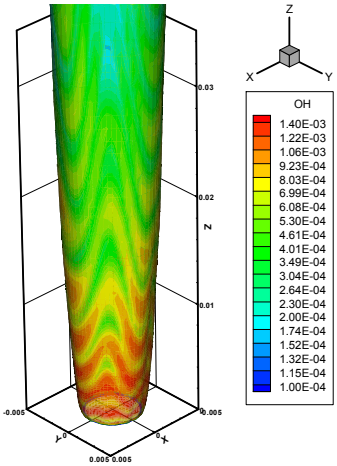

b. Contour of OH, $\xi = 0.037$

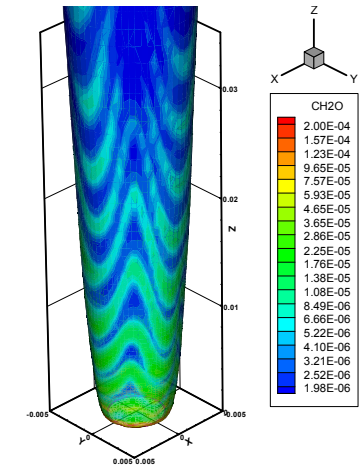

c. Contour of CH_2O, $\xi = 0.015$

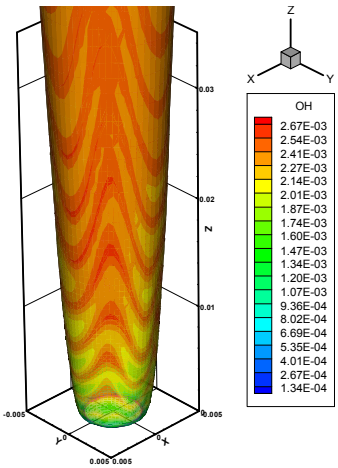

d. Contour of OH, $\xi = 0.015$

Figure 6. Contour of CH_2O and OH on isosurface of mixture fraction for 9% O_2 coflow.

results, OH radical is known as a flame marker and the concentration of CH_2O radical is mostly predominant at zones where re-ignition in flame occurs. In addition to OH, Najm et al. [22] reported that the HCO radical is also related to chemical heat release. Therefore, the contour of mean CH_2O and mean HCO are presented in the Figs. 5.c and 5.d respectively. The same behavior can be seen from this figures obviously. The presence of discontinuity at HCO and CH_2O again proves that some local extinction and re-ignition are existed specially near the fuel nozzle exit zone. CH_2O distribution in the downstream of flow is smoother than near the nozzle exit zones. Considering these observations, local extinctions and reigniting are more intensive and periodic in upstream. It should be noted that by going forward along the centerline, the distance between two different depicted mixture fraction lines will be greater. In order to studying theses physical phenomenon more carefully, all data are extracted on two mixture fraction isosurface, 0.037 and 0.015, along the Z direction up to 30 mm in Figs. 6.a and 6.b. Fig. 6.a is related to stoichiometric mixture. On each of these isosurfaces the contours of mean OH and mean CH_2O are illustrated. Periodic distributions of OH and CH2O can be seen from these figures. These figures show that, oscillations of OH and CH_2O mass fraction are intensified near the jet exit and are decayed along the center line. As can be seen, the existence of these extinction and re-ignition zones are a fully 3-D phenomenon and cannot be considered as 2-D one.

The counters of , Fig. 5.b, is shown to investigate the influence of turbulence on local flame suppression. The factor κ, similar to radical OH, shows some kind of discontinuity. The minimum value of κ occurs where the OH mass fraction has the maximum quantity. Its reason is related to definition of τ_{mix}. Increasing κ (decreasing τ_{mix}) causes increasing the mixing unburned species with burned ones. This increase consequently decrease the final species temperature and OH mass fraction.

Results for 3% O_2

Since O_2 mass fraction is an influential parameter in studying the MILD combustion regime, effects of decreasing the O_2 mass fraction of coflow jet on flame structure are investigated. In Figs. 7.a and 7.b contours of mean OH radical and κ are illustrated for 3% O_2 coflow. Similar to Figs. 6.a and 6.b, two mixture fraction lines For two values of 0.0259 and 0.00269 are illustrated in Figs 8.a and 8.b. The mixture fraction of 0.0259 is the stoichiometric mixture fraction and the later on, 0.00269, is related to where the OH radical is approximately maximum(i.e. reaction zone). Moreover the contours of mean CH_2O and HCO mean are illustrated in Fig. 7.c and 7.d, respectively.

Comparison between two contour of OH for 3% and 9% O_2 imply that, the flame zone is thickened to provide necessary oxygen. Such an idea could arise from the relatively larger distance between stoichiometric mixture fraction positions and the intense reaction zone (the related iso-mixture line) for 3% O_2 in comparison with 9% O_2. It is in consistency with the main characteristic of MILD combustion on larger reaction zone which has been introduced by many other reports [4,5,6]. Again similar to 9% O_2, the mentioned phenomena related to flame local extinction and re-ignition could be concluded from the Fig. 7, although the concentration of species are reduced as a result of lower reaction rates in more diluted conditions, 3% O_2. In order to study the effect of oxygen level on the above mentioned phenomena, the isosurfaces of mixture fraction for two value of stoichiometric are shown in Fig. 8. The contours of OH and CH_2O are depicted in these isosurfaces. Comparing the Figs. 6 and 8 could reveal some points as follows; first the reaction zone at upstream takes place around the condition of stoichiometric, although it is going to deviate from stoichiometric condition at far from the nozzle and in downstream. Such a deviation is happen more quickly at lower oxygen level as results of more distributed reaction zone. Second, although extinction

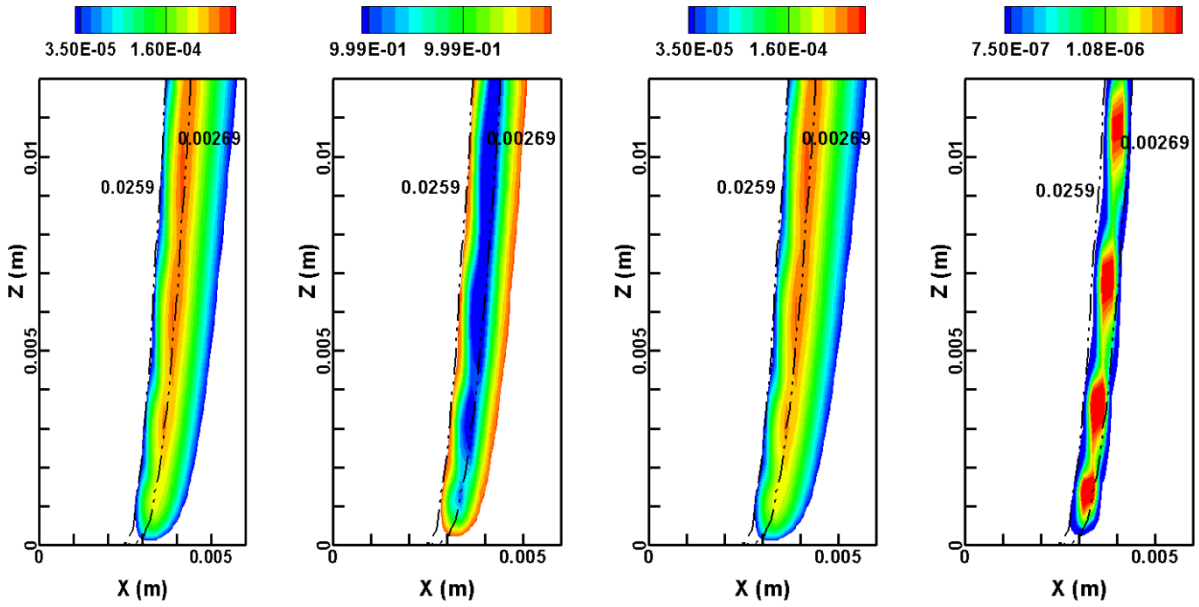

a. Contour of OH **b**. Contour of κ **c**. Contour of CH_2O **d**. Contour of HCO

Figure 7. Contour of κ and three other species mass fraction for 3% O_2 coflow

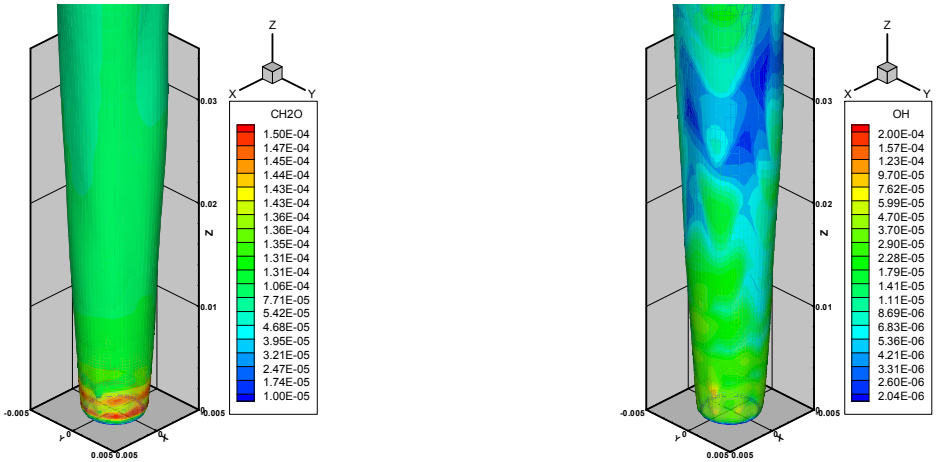

a. Contour of CH_2O, $\xi = 0.0259$ **b.** Contour of OH, $\xi = 0.0259$

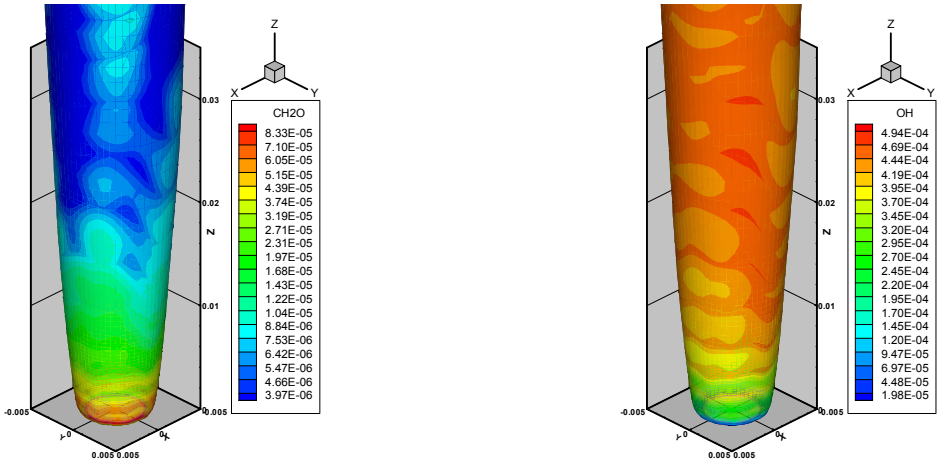

c. Contour of CH_2O, $\xi = 0.00269$ **d.** Contour of OH, $\xi = 0.00269$

Figure 8. Contour of CH_2O and OH on isosurface of mixture fraction for 3% O_2 coflow.

and re-ignition phenomena occur for both 3 and 9 % O_2 levels, they are more intense in larger O_2 concentrations. Comparing Figs. 6.d and 8.d illustrate that for 3% O_2 the OH contours are more uniform in comparison with 9% O_2. In other word the extinction and re-ignition are present in a larger volume of reaction zone with a smoother intensity at lower Reynolds number.

Conclusion

In this paper, the MILD combustion modeling using the LES and detailed chemical mechanism is done to investigate some main characteristics of this combustion regime. In this way, OpenFOAM code with its LES sub-models are used to model flow dynamic. Furthermore the interaction between turbulence and chemical reactions are considered by the PaSR model which accompanied with the DRM-22 chemical mechanism.

Results illustrate that the measured temperature and species distribution, in experiments, are predicted in current LES modeling with an acceptable accuracy. Furthermore, the main features of MILD combustion such as flame extinction and re-ignition and flame sensitivity to oxidizer oxygen concentration are captured by the current numerical approach. The flame structure is illustrated by studying of the local concentrations of some minor species like OH, CH_2O, and HCO. Decreasing of oxygen concentration leads to larger and more uniform reaction zone. Moreover the extinction and re-ignition occur in larger area and with lower intensity at lower oxygen levels under MILD combustion condition.

References

[1] Cavalier, A., de Joannon, M., "Mild combustion", *Prog. Energy Combust. Sci.* 30: 329-366 (2004)

[2] Dally, B.B., " Laminar nonpremixed flame calculations of methane with highly preheated air", *The 1999 Australian Symposium on Combustion & Sixth Australian Flame Days*, Newcastle, Australia (1999)

[3] Dally, B. B., Karpetis, A.N., Barlow, R.S., "Structure of turbulent non-premixed jet flames in a diluted hot coflow" *Proc. Combust. Inst* 29: 1147-1154 (2002).

[4] Christo, F.C., Dally, B.B., "Modeling turbulent reacting jets issuing into a hot and diluted coflow", *Comb. and Flame* 142: 117-129 (2005)

[5] Frassoldati, A., Sharma, P., Cuoci, A., Faraveli, T., Ranzi, E., "Kinetic and fluid dynamics modeling of methane/hydrogen jet flames in diluted coflow", *Applied Thermal Engineering* 30: 376-383 (2010)

[6] Mardani, A., Tabejamaat, S., Ghamari, M., "Numerical study of influence of molecular diffusion in the Mild combustion regime" *Combustion Theory and Modeling* Vol.14, No.5: 747-774 (2010)

[7] Ihme, M., See C.Y., "LES flamelet modeling of a three stream MILD combustor: Analysis of flame sensitivity to scalar inflow conditions" *Proc. Combust. Inst* 33: 1309-1317 (2011).

[8] Kobayashi, H., Oono, K., Cho, E.S., Hagiwara, H., Ogami, Niioka, T., "Effects of turbulence on flame structure and NOx emission of turbulent jet non-premixed flames in high-temperature air combustion" *JSME International Journal* Series B, Vol. 48, No.2 (2005)

[9] Medwell, P.R., Kalt, P.A.M., Dally, B.B., "Influence of fuel type on turbulent nonpremixed jet flames under MILD combustion conditions" *16th Australian Fluid Mechanics Conference*: 1350-1355 (2007)

[10] Magnussen, B.F., "On the structure of turbulence and a generalized eddy dissipation concept for chemical reaction in turbulent flow, 19th AIAA Meeting, St. Louis, MO (1981)

[11] Chomiak, J., Karlsson, J., "New observations concerning diesel combustion" Proceddings of the 22nd CIMAC, Vol. 2: 431-441 (1998)
[12] Smagorinsky, J.S., "General circulation experimental with the primitive equations", *Monthly Weather Review*, Vol. 91, No. 3: 99-165 (1963)
[13] Poinsot, T., Veynant, D., *Theoretical and numerical combustion*, Edwards, 2005, p. 252
[14] Weller, H.G., Tabor, G., Jasak, H., Fureby, C., "A tensorial approach to computational continuum mechanics using object-oriented techniques", Computer in Physics, Vol. 12, NO. 6: 620-631 (1998)
[15] Issa, R.I., "Solution of the implicity discretized fluid flow equations by operator splitting", *J. Computational Physics* 62: 40-65 (1986)
[16] Peng Karrholm, F., "Numerical modeling of diesel spray injection and turbulence interaction" Department of Applied Mechanics, Chalmers University of Technology (2006)
[17] Kazakov, A., Frenklach, M., "Reduced reaction sets based on GRIMech1.2. [Available at http://www.me.berkeley.edu/drm/
[18] Frenklach, M., Wang, H., Yu, C-L., Goldenberg, M., Bowman, C.T., Hanson, R.K., et al. GRI-1.2. [Available athttp://www.me.berkely.edu/gri_mech/].
[19] Klein, M., "An attempt to assess the quality of large eddy simulations in the contex of implicit filtering" *Flow, Turbulence and Combustion* 75: 131-147 (2005)
[20] Pope, S., "Ten questions concerning the large eddy simulation of turbulent flows" *New J. Phys. 6* (2004)
[21] Bilger, R.W., Starner, S.H., Kee, R.J., "On reduced mechanisms for methane-air combustion in non-premixed flames" *Combust. Flame* 80: 135-149 (1990)
[22] Najm, H.N., Paul, C.J., Wyckoff, P.S., "On the adequacy of certain experimental observables as measurements of flame burning rate" *Combust. Flame* 113: 312-332 (1998)